Naval Research Laboratory

Washington, DC 20375-5320

NRL/MR/5303--95-7743

Ambient Light Calibration of a Scanning Slope Sensor

MARK A. SLETTEN
DENNIS B. TRIZNA

Senior Scientist and Propagation Staff
Radar Division

PAUL A. HWANG

QUEST Integrated, Inc.,
Kent, WA

June 26, 1995

REPORT DOCUMENTATION PAGE

Form Approved
OMB No. 0704-0188

1. AGENCY USE ONLY (*Leave Blank*)	2. REPORT DATE	3. REPORT TYPE AND DATES COVERED
	June 26, 1995	

4. TITLE AND SUBTITLE

Ambient Light Calibration of a Scanning Slope Sensor

5. FUNDING NUMBERS

PE-61153N
PR-RR021-05-AG
WU-53-3620-A5

6. AUTHOR(S)

M. Sletten, P. Hwang, and D. Trizna

7. PERFORMING ORGANIZATION NAME(S) AND ADDRESS(ES)

Naval Research Laboratory
Washington, DC 20375-5320

8. PERFORMING ORGANIZATION REPORT NUMBER

NRL/MR/5303--95-7743

9. SPONSORING/MONITORING AGENCY NAME(S) AND ADDRESS(ES)

Office of Naval Research
800 North Quincy Street
Arlington, VA 22217-5660

10. SPONSORING/MONITORING AGENCY REPORT NUMBER

11. SUPPLEMENTARY NOTES

12a. DISTRIBUTION/AVAILABILITY STATEMENT

Approved for public release; distribution unlimited.

12b. DISTRIBUTION CODE

13. ABSTRACT (*Maximum 200 words*)

This paper outlines a procedure developed to calibrate a laser-based water surface slope sensor against ambient light variations. An analysis of the optical position sensor used in the system indicates how variations in the ambient light intensity cause shifts in the illumination pattern centroid calculated by the sensor electronics. These shifts are misinterpreted as slope variations of the water surface unless special calibration measures are performed. The analysis is also used to illustrate a technique to compensate for this effect. The analysis is validated using laboratory and field data, and the calibration technique is then applied to data recently collected in the North Atlantic during the joint **ONR/NRL HIRES** program.

14. SUBJECT TERMS

15. NUMBER OF PAGES

26

16. PRICE CODE

17. SECURITY CLASSIFICATION OF REPORT	18. SECURITY CLASSIFICATION OF THIS PAGE	19. SECURITY CLASSIFICATION OF ABSTRACT	20. LIMITATION OF ABSTRACT
UNCLASSIFIED	UNCLASSIFIED	UNCLASSIFIED	UL

NSN 7540-01-280-5500

Standard Form 298 (Rev. 2-89)
Prescribed by ANSI Std 239-18
298-102

Table of Contents

AMBIENT LIGHT CALIBRATION OF A SCANNING SLOPE SENSOR

1. Introduction

In both the study of air-sea interactions and in microwave remote sensing of the ocean surface, wind generated roughness plays a central role. Momentum exchange between wind and water generates capillary-gravity (CG) waves, which in turn serve as the progenitors of the longer wave field. Large and small scale wave breaking contributes to the transfer of gases from the atmosphere to the sea. In radar remote sensing, the ripples, cusps and breakers generated by the wind serve as the electromagnetic scattering centers and carry information on the winds, currents, and surfactants.

In both areas of research, an accurate measure of the sea surface morphology is crucial to a true understanding of the physics at work. Various methods have been used in the past to measure and characterize the ocean surface. In the classic work of Cox and Monk (1954), sun glitter in aerial photographs was used to determine the relationship between the mean square slope of the surface and wind speed. Wire wave gauges have used for many years to measure the temporal behavior of the surface height at a single point. The laser slope gauge, in which the refraction of a laser beam at the air-sea interface is used to determine the surface slope, can also be used in a similar, single-point mode while allowing the measurement of considerably shorter waves.(Palm et al. 1977; Hughes et al. 1977; Hughes and Grant 1978; Hughes and Gower 1983; Tang and Shemdin 1983; Hwang and Shemdin 1988; Shemdin and Hwang 1988). While these gauges can provide a satisfactory measure of the frequency spectrum of the surface, the conversion to wavenumber is difficult, particularly under field conditions, due to the advection of CG waves by longer waves. Blockage and wave breaking also present considerable problems when attempting to convert

Manuscript approved April 18, 1995.

frequency spectra to wavenumber spectra. Recently, scanning laser slope sensors have been developed which attempt to circumvent the frequency to wavenumber conversion by directly measuring the two-dimensional slope structure. Researchers at TRW were the first to develop such an instrument for open ocean use, but little data is available in the open literature (Lee et al. 1992). Martinsen and Bock (1992) have also developed a system, mounted on a pontoon, and the results of an experiment in which the system was moored off a dock at the Woods Hole Oceanographic Institute have recently been published (Hara et al. 1994). A third system, referred to as the Scanning Slope Sensor (SSS), has recently been developed and is mounted on a free-drifting buoy. This system was successfully deployed in the North Atlantic in 1993, and an analysis of some aspects of the rich data set collected during this experiment has been reported (Hwang et al., 1994).

In any of these optical sensors under field conditions, ambient light generated by the sun constitutes a noise source. In the open ocean, sunlight can easily saturate or at least corrupt the detector output, even when narrowband filters, tuned to the laser wavelength, are employed. This effect must be removed if accurate measures of surface slope are to be obtained. Bock (private communication) has implemented a hardware solution to this problem in which the ambient contribution to the detector output is reduced before sampling and recording. This approach has the advantage of speed, but at the cost of additional sampling capabilities and other electronics.

In this paper, a different technique is described. A software calibration algorithm has been developed for the SSS buoy which compensates for variations in the sensor output caused by ambient light fluctuations. The technique is advantageous in that all quantities

needed for the calibration are derived from the raw data itself. A separate experiment to measure the ambient light sensitivity of the instrument is unnecessary, and any fluctuations in the signal level, produced by changing environmental conditions, are inherently accounted for. The technique has proven to be effective for ambient light levels up to the moderate levels commonly encountered during open ocean deployments.

This paper is organized into six sections. Section 2 contains a description of the SSS hardware. In Section 3, the basis for the ambient light calibration procedure is derived through an analysis of the operation of the optical position sensor. This analysis is validated using both laboratory and open ocean data in Section 4, while Section 5 contains examples of the data collected during the 1993 North Atlantic deployment. A summary is presented in Section 6.

2. Description of the Scanning Slope Sensor

Figure 1 contains two photographs of the SSS system. The system electronics and optics are housed in two waterproof canisters, and a floatation system positions the mean water surface approximately midway between the two during deployment. The optical portion of the slope sensor consists of a red laser (670 nm wavelength, 8 mW output), lens, and a 24 facet rotating mirror housed in the lower container and an optical x-y position sensor positioned in the upper unit. The beam produced by the diode laser is directed through the lens to the rotating mirror where angled facets scan the beam through a wedge shaped volume. After a second pass through the lens, a raster scan pattern consisting of 8 parallel lines, 10 cm in length spaced 0.5 cm apart, is produced at the water surface . The

water/air interface causes the beam to refract at an angle with respect to the vertical direction and causes a displacement $\Delta r=\sqrt{\Delta x^2+\Delta y^2}$ of the laser spot on the x-y detector relative to its calm water position. This displacement and the instantaneous surface elevation (measured by pressure sensors mounted 30 cm below the mean water level) are used to determine the slope at the point at which the laser beam intercepts the surface. A data acquisition system housed in the lower waterproof canister samples the detector output at 50 points along each of the 8 parallel scans. The central 32 points from each scan are used to produce an 8x32 image of the surface slope. A single 8x32 image (frame) is typically collected in 34 ms for a frame rate of approximately 30 Hz. The SSS system includes sufficient memory (RAM) to allow collection of 256 contiguous frames, approximately 9 s of data, before pausing to write to an on-board disk drive. Additional software overhead results in a total cycle time of approximately 10 s per 256 frame data segment.

The SSS buoy also supports a number of additional sensors. Air and sea temperature are recorded by temperature probes mounted 0.97 m above and 0.47 m below the mean sea surface, respectively. Wind speed and direction are monitored in two locations, at 1.33 m and 1.05 m above the surface, allowing for the determination of wind stress. A magnetic compass is used to monitor the orientation of the system, and a set of three accelerometers allows monitoring of motions induced by longer waves. The support structure for the system consists of a 5 m long frame with a triangular cross section (Fig. 1). The buoy is operated in a free-drifting mode to reduce the relative velocity between the surface current and the sensor, thus minimizing flow distortion in the sensing area. A wind vane orients one of the broad sides of the structure into the wind to further reduce distortion.

3. Effect of Ambient Light on Slope Measurements

The relationship between the displacements Δx and Δy , the surface elevation, and the surface slope can be derived through Snell's Law (Palm et al., 1977; Hughes et al., 1977; Tang & Shemdin, 1983; Hwang & Shemdin, 1988; Hwang et al., 1993). *Calibration* of the system consists primarily of relating the measured position sensor outputs (in volts) to the displacements Δx and Δy (in cm). However, this procedure is complicated by the fact that the proportionality constant is a function of the ambient light intensity. The detector determines the laser spot position by calculating the centroid of the light pattern projected on it. Changes in the ambient light level produce changes in the centroid and thus corrupt the position measurement. This effect is correctable, however, in the following manner. In lateral effect photodiodes of the type used in the position sensor, the normalized position is derived from currents, I_1, I_2, induced in terminals located on opposite sides of the light collection region. Each current is the weighted integral of the intensity pattern on the photodiode surface, the weight being inversely proportional to the distance between the terminal and the current element. Specifically,

$$I_1 = A\int_0^L (L-x)\cdot\Phi(x)\,dx \qquad I_2 = A\int_0^L x\cdot\Phi(x)\,dx \qquad \text{(1a,b)}$$

where the total length of the device is assumed to be L, its responsivity is A, and the intensity pattern is given by $\Phi(x)$. Given that the detector looks down at a frosted glass image plane; the ambient pattern can be approximated by a uniform intensity $\Phi_{ambient}$.

Modeling the laser pattern by a spot of width Δ, location x_o, and intensity Φ_{laser} yields

$$\Phi(x) = \Phi_{ambient} + \Phi_{laser}[U(x-x_o+\Delta/2) - U(x-x_o-\Delta/2)] \qquad (2)$$

where $U(x)$ is the unit step function. The simple integrations indicated by Eqs. 1a,b then produce the following terminal currents:

$$I_1 = \frac{A\Phi_{ambient}L^2}{2} + A\Phi_{laser}\Delta(L-x_o) \qquad I_2 = \frac{A\Phi_{ambient}L^2}{2} + A\Phi_{laser}\Delta x_o . \quad (3a,b)$$

The centroid of the pattern is calculated by electronics within the detector assembly as

$$\hat{x} = \frac{I_1-I_2}{I_1+I_2} = \frac{\Phi_{laser}\Delta(L-2x_o)}{\Phi_{ambient}L^2+\Phi_{laser}\Delta L} . \qquad (4)$$

This quantity is converted to a voltage and then sampled by the SSS system. The ratio of the measured centroid to that measured if the ambient level were zero ($\Phi_{ambient}=0$) can be written as

$$\frac{\hat{x}}{\hat{x}_o} = \frac{\Phi_{laser}\Delta L}{\Phi_{ambient}L^2+\Phi_{laser}\Delta L} = \frac{S}{S+N} = \frac{R}{1+R} \qquad (5)$$

where S is the signal produced by the laser, N is the noise produced by the ambient, and R is the signal to noise ratio.(See also Hwang et al. 1994) This function is plotted in Figure 2a, assuming a typical signal level of 2 volts. Note the monotonic decrease in the detector output as the ambient level is increased. Without compensation, this effect will cause

significant errors in the determination of the displacements and thus in the slope measurements. Note also, however, that $\hat{x}/\hat{x}_o$ is independent of the laser spot position and is a constant for a given signal to noise ratio. If this quantity can be measured for any laser position under a given set of signal and ambient conditions, the detector outputs can be re-scaled and the slope measurements corrected. This is the principle behind the calibration procedure. In practice, a calibration factor proportional to $\hat{x}/\hat{x}_o$ is calculated from an estimate of the "calm-water" output of the detector, and this calm-water pattern is computed from a time average of the raw data itself. This procedure and a validation of the analysis presented above are presented in the next section.

4. Validation of the Calibration Procedure

Both laboratory and field data were analyzed in order to test the validity of the ambient light analysis. In the laboratory experiments, the sensor was placed in an enclosure containing a variable intensity white light source. The position sensor output was then recorded as a function of the ambient light intensity, the latter of which is also derived from the detector outputs. Figure 2b shows the results of the test. The normalized output of the position sensor for a laser beam displacement of 6 cm is plotted vs the ambient level. The data agrees with the theoretical analysis of Figure 2a quite well, although the agreement depends in part on the exact value of the signal produced by the laser alone (assumed to be 2 v in the analysis of Figure 2a), and this quantity was not measured during these experiments. Subsequent measurements of the signal level place it in the 1-2 volt range, however. There appears to be a saturation effect in the laboratory data above an ambient level of

approximately 4 volts, so application of the calibration technique to field data was consequently limited to data sets with ambient light levels less than this amount.

In order to verify the analysis of the ambient light effect under field conditions, open ocean data were analyzed as well. In June of 1993, the SSS was deployed in the Atlantic off the coast of Cape Hatteras as part of the joint ONR/NRL High-Resolution Remote Sensing Accelerated Research Initiative (HI-RES ARI). Over a two week period, a rich data set was collected under low ambient light levels and a variety of wind and sea conditions. An analysis of some aspects of this data set have been reported recently (Hwang et al., 1994). Unlike the laboratory data, which was collected in the absence of any water or waves, the field data must be pre-processed before the effects of ambient light can be determined. In order to remove the effects of water waves and isolate any ambient light effects, the calm-water output from the position sensor was first estimated by averaging raw data over 9 second intervals. Under the reasonable assumption that the mean slope at any point on the surface is zero over the 9 s averaging period, this process effectively removes the laser beam displacements caused by surface waves, and thus the resulting signal pattern is the same as that produced under calm water conditions.(See Fig. 3 below) The detector output for any given displacement can be determined from this pattern, and thus the calibration factor can be computed for the particular signal and ambient light levels present during the 9 s segment. Only data sets for which the light levels were relatively constant over the averaging interval were considered for this processing.

Figure 3 illustrates the averaging procedure. A typical raw output signal for a single eight-line frame is shown along with the pattern produced by averaging over 256 such frames

(9 seconds of data). The sharp peaks seen in the raw data, caused by points of high slope on the surface, are removed through the averaging process, and the sawtooth pattern produced by the detector under calm conditions can be seen clearly. The eight segment sawtooth pattern is a result of the eight linear laser scans comprising a single frame. The peak to peak voltage swing of each segment corresponds to a 6 cm shift in the laser spot position. The ratio of this voltage swing to the 6 cm displacement is the calibration factor required to relate the detector output to the true laser beam displacement. This factor is proportional to the ratio $\hat{x}/\hat{x}_o$ defined in Eq. (5).

Figures 4a-d show the results of the ambient light analysis of the open ocean data. The detector output for a displacement of 6 cm is plotted vs the ambient level. (The normalized output is not plotted, as in Figures 2 and 3, since the 0 v ambient condition was not encountered and thus the normalization constant could not be determined.) In each of the four cases shown, the data shows the predicted monotonic decrease in the signal with increasing ambient level. Gaps appear in some of these figures since all ambient levels were not present for all four runs due to day-to-day variations in cloud cover and differences in the time of day of each deployment. During two other runs (data not shown), the ambient level varied little and thus the decrease is not apparent. The means and error bars ($\pm\sigma$) indicated in the figures were computed by first separating the data into 0.25 v wide (ambient level) bins. The total number of data points comprising each figure ranges from 426 to 721.

The apparent vertical shifts of the data from run-to-run (between files 1213 and 1413, for example) have two possible causes. First, adjustments in the buoy flotation system over the course of the experiment may have caused changes in the mean distance, in water,

traversed by the laser beam. This, in turn, may have caused changes in the attenuation of the laser signal. Second, changes in the water clarity itself may have also caused shifts in the signal level. Note, however, that these variations will not effect the quality of the ambient light compensation scheme, even if they occur during the course of any one deployment: Each 9 s segment of data is calibrated with a constant computed from that data segment itself, and thus signal level variations are inherently accounted for. (These variations must occur on a time scale which is long compared to the 9 second averaging time, however.)

5. Example Data from the North Atlantic

Some of the capabilities of the SSS system are illustrated in Figures 5 and 6 where additional data from the 1993 HI-RES field experiment is displayed. Figure 5 illustrates the system's ability to measure the fine, dynamic structure of the sea surface. This figure is a grey-scale image of the surface curvature, the spatial derivative of the surface slope, calculated by taking the difference of adjacent slope samples. The calculation and display of curvature, rather than slope, highlights the fine surface structure and improves the accuracy of spectral estimation techniques.(Hwang et al. 1994) 256 contiguous frames of data are concatenated and arranged in 8 parallel columns. Time increases from bottom to top and from left to right. (Column 1 contains the first 32 frames, column 2 the second 32, etc.) The passage of wind driven waves through the scanning region produces the mottled regions seen in the figure. Wave velocity relative to the SSS system produces the diagonal orientation of some of the mottled regions, as seen near the bottom of column 4. The

vertical bands formed by wave crests and troughs in the upper half of column 8 indicate a feature nearly stationary with respect to the SSS system. Quantitative information on these motions and on the spectral characteristics of the fine structure can be obtained through a straightforward application of a Fast Fourier Transform.

On several occasions during the HI-RES experiment, internal waves (IWs) were encountered and sampled by a variety of instruments. These subsurface disturbances alter the surface morphology through wave-current interactions, and the modulation in radar backscatter this produces has been studied by many researchers. (See, for example, *J. Geophys. Res.* **93**, no.C10, 1988.) Figure 6 displays data collected while the SSS system was drifting in a region in which IW bands were clearly visible on the ship's navigation radar. In 6a, the water temperature as measured by the SSS system is plotted versus time, and the passage of the system through a surface manifestation of the IW is indicated by the temperature dip near t=3250 s. Figure 6b displays the corresponding rms surface curvature as measured by the slope sensor. Significant increases in the rms curvature, on the order of 100 %, can be seen on both sides of the dip. Efforts are underway to characterize the scatterers responsible for these increases in roughness and to reconcile the SSS data with the radar images of the IW. While a full interpretation of these results is beyond the scope of this paper and will be reported elsewhere, this data is presented here to illustrate some of the unique capabilities of the SSS system.

6. Summary

In this paper, a software technique is outlined which removes the effect of ambient

light variations on the measurements produced by a scanning laser slope sensor. The operation of the optical position sensor is analyzed to show the mechanism by which the signal is degraded. The sensor interprets the centroid of the intensity pattern as a measure of the position of the laser beam, but the centroid is a function of the ambient light level. The analysis also indicates that the proper signal can be recovered by scaling the sensor output with a calibration factor obtainable from the data itself through an averaging technique. Laboratory and open ocean data are analyzed to validate the procedure. Some of the capabilities of the SSS system are illustrated with data collected in the North Atlantic as part of the HIRES ARI program.

References

Cox, C.S., and Munk, W., 1954: Statistics of the Sea Surface Derived from Sun Glitter. *J. Mar. Res.* **13**, 198-227.

Hara, T., Bock, E.J., and Lyzenga, D., 1994: In Situ Measurements of Capillary-Gravity Wave Spectra Using a Scanning Laser Slope Gauge and Microwave Radars. *J. Geophys. Res.* **99**, 12,593-12,602.

Hughes, B.A. and Grant, H.L., 1978: The Effect of Internal Waves on Surface Wind Waves. 1. Experimental Measurements. *J. Geophys. Res.* **83**, 443-454.

Hughes, B.A. and Gower, J.F.R., 1983: SAR Imagery and Surface Truth Comparisons of Internal Waves in Georgia Strait, British Columbia, Canada. *J. Geophys. Res.* **88**, 1809-1824.

Hughes, B.A., Grant, H.L., and Chappell, R.W., 1977: A Fast Response Surface-wave Slope Meter and Measured Wind-Wave Moment. *Deep-Sea Res.* **24**, 1211-1223.

Hwang, P.A. and Shemdin, O.H., 1988: The Dependence of Sea Surface Slope on Atmospheric Stability and Swell Conditions. *J. Geophys. Res.* **93**, 13903-13912.

Hwang, P.A., Trizna, D.B., and Wu, J., 1993: Spatial Measurements of Short Wind Waves

Using a Scanning Slope Sensor. *Dyn. Atm. Oceans* **20**, 1-23.

Hwang, P.A., Atakturk, S., Sletten, M.A., and Trizna, D.B., 1994: A Study of the Wavenumber Spectrum of Capillary-Gravity Waves. submitted to *J. Fluid Mech.*

Lee, P.H.Y., Barter, J.D, Beach, K.L., Hindman, C.L., Lake, B.M., Rungaldier, H., Schatzman, J.C., Shelton, J.C., Wangner, R.N., Williams, A.B., Yee, R., and Yeun, H.C., 1992: Recent Advances in Ocean Surface Characterization by a Scanning Laser Slope Gauge. *Optics of the air-sea interface: Theory and measurement*, SPIE **Vol. 1749**, 234-244.

Martinsen, R.J. and Bock, E.J., 1992: Optical Measurements of Ripples Using a Scanning Laser Slope Gauge. Part I: Instrumentation and Preliminary Results. *Optics of the air-sea interface: Theory and measurement*, SPIE **Vol. 1749**, 258-271.

Palm, C.S., Anderson, R.C., and Reece, A.M., 1977: Laser Probe for Measuring 2-D Wave Slope Spectra of Ocean Capillary Waves. *Appl. Opt.* **16**, 1074-1081.

Shemdin, O.H. and Hwang, P.A., 1988: Comparison of Measured and Predicted Sea Surface Spectra of Short Waves. *J. Geophys. Res.* **93**, 13883-13890.

Tang, S. and Shemdin, O.H., 1983: Measurements of High Frequency Waves Using a Wave Follower. *J. Geophys. Res.* **88**, 9832-9840.

Figure Captions

1. Photographs of the SSS system showing a) the upper and lower waterproof canisters and the triangular support frame, and b) the system in operation.

2. a) Plot of the normalized position sensor output versus the ambient light level as predicted by Eq. 5. A signal level of 2 v is assumed. b) Plot of the normalized position sensor output versus the ambient light level as measured under laboratory conditions.

3. Single frame of open-ocean data from the position sensor and the pattern produced by the 9 s (256 frame) averaging procedure.

4. Position sensor output signal vs ambient light intensity for four open-ocean deployments of the SSS system. The means and error bars were computed on the basis of 0.25 v (ambient level) bins.

5. Typical grey-scale image of the surface curvature measured during the North Atlantic deployment. 256 contiguous frames are shown in the eight parallel columns.

6. SSS system data collected in the presence of internal waves. a) Water temperature versus time, b) corresponding rms surface curvature.

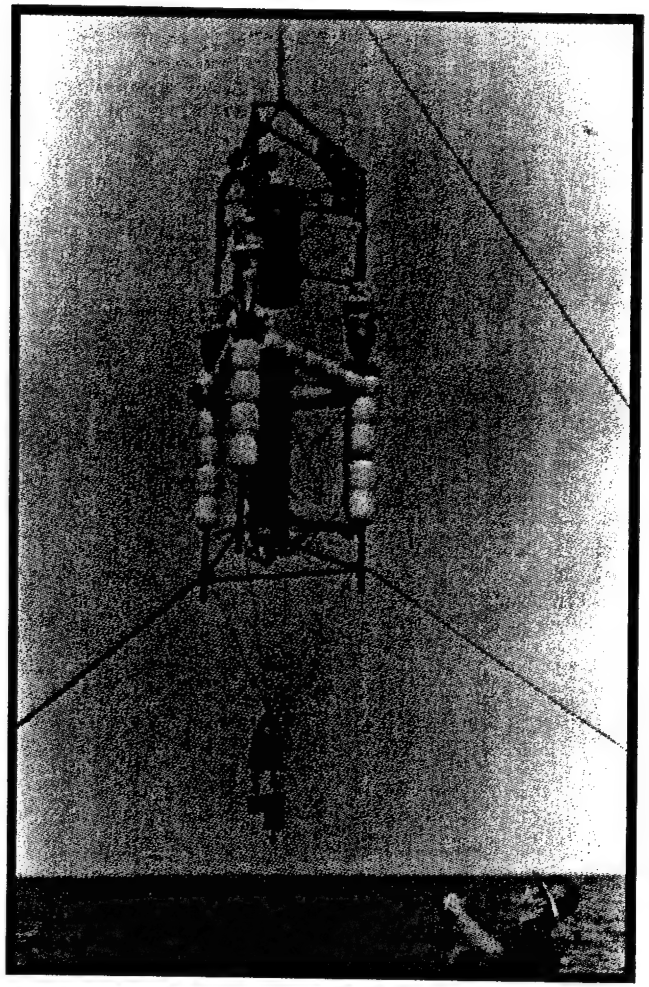

a)

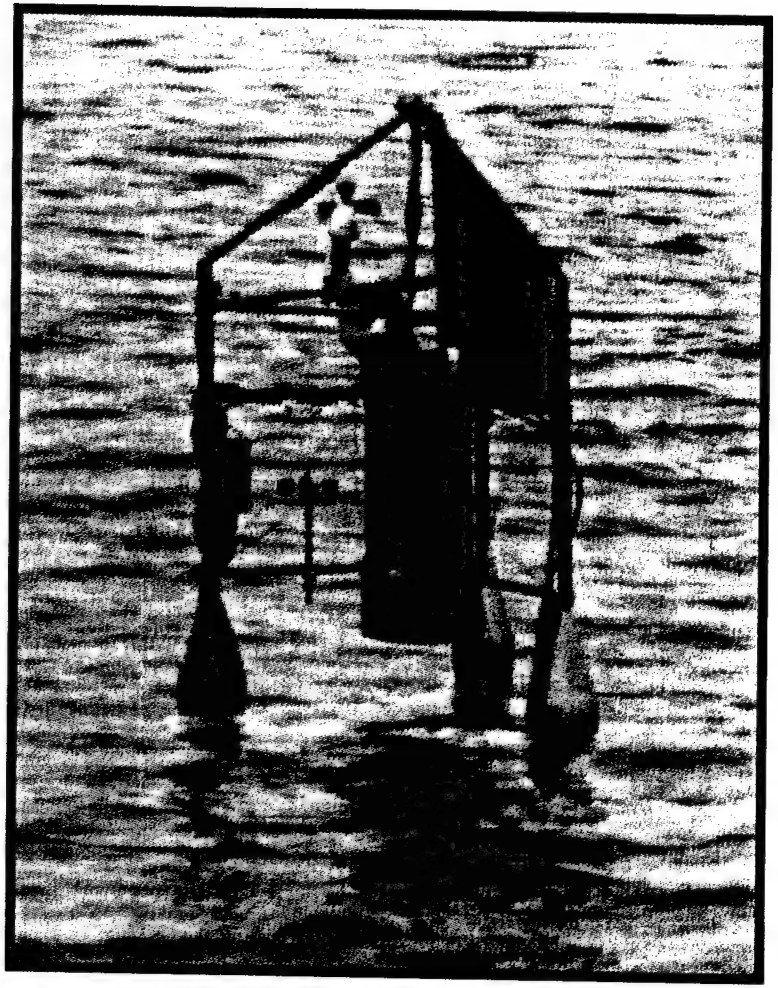

b)

1. Photographs of the SSS system showing a) the upper and lower waterproof canisters and the triangular support frame, and b) the system in operation.

a)

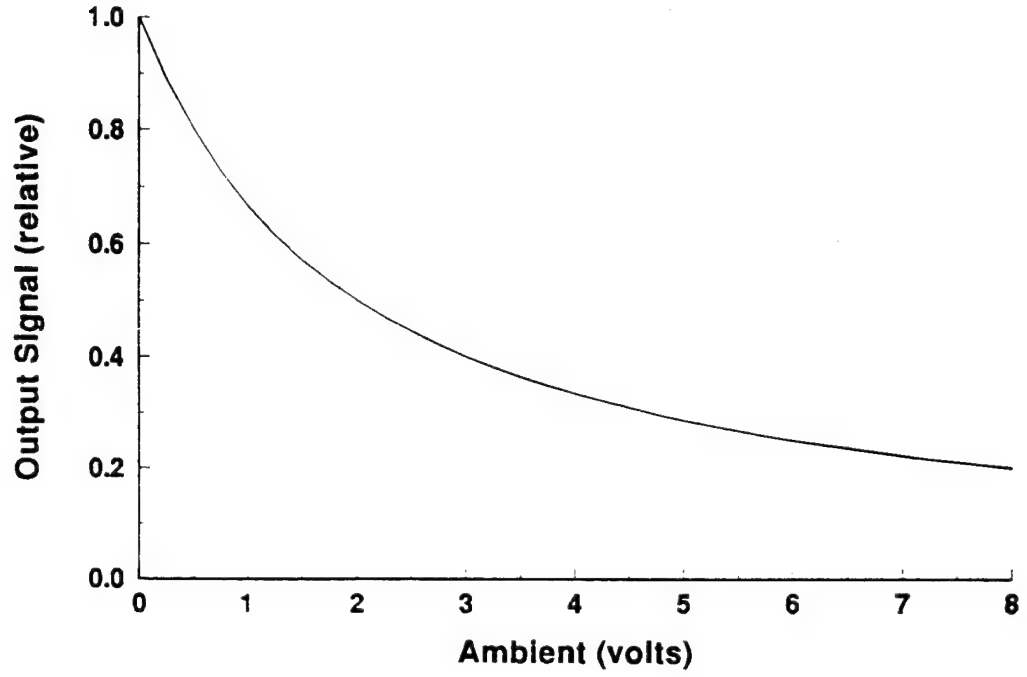

b)

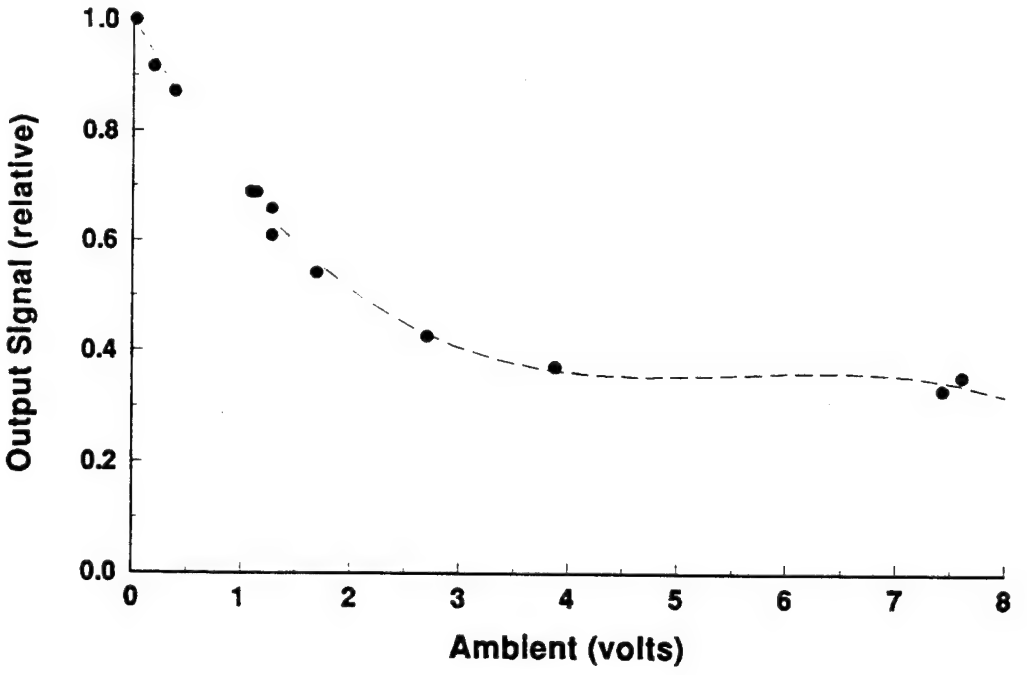

2. a) Plot of the normalized position sensor output versus the ambient light level as predicted by Eq. 5. A signal level of 2 v is assumed. b) Plot of the normalized position sensor output versus the ambient light level as measured under laboratory conditions.

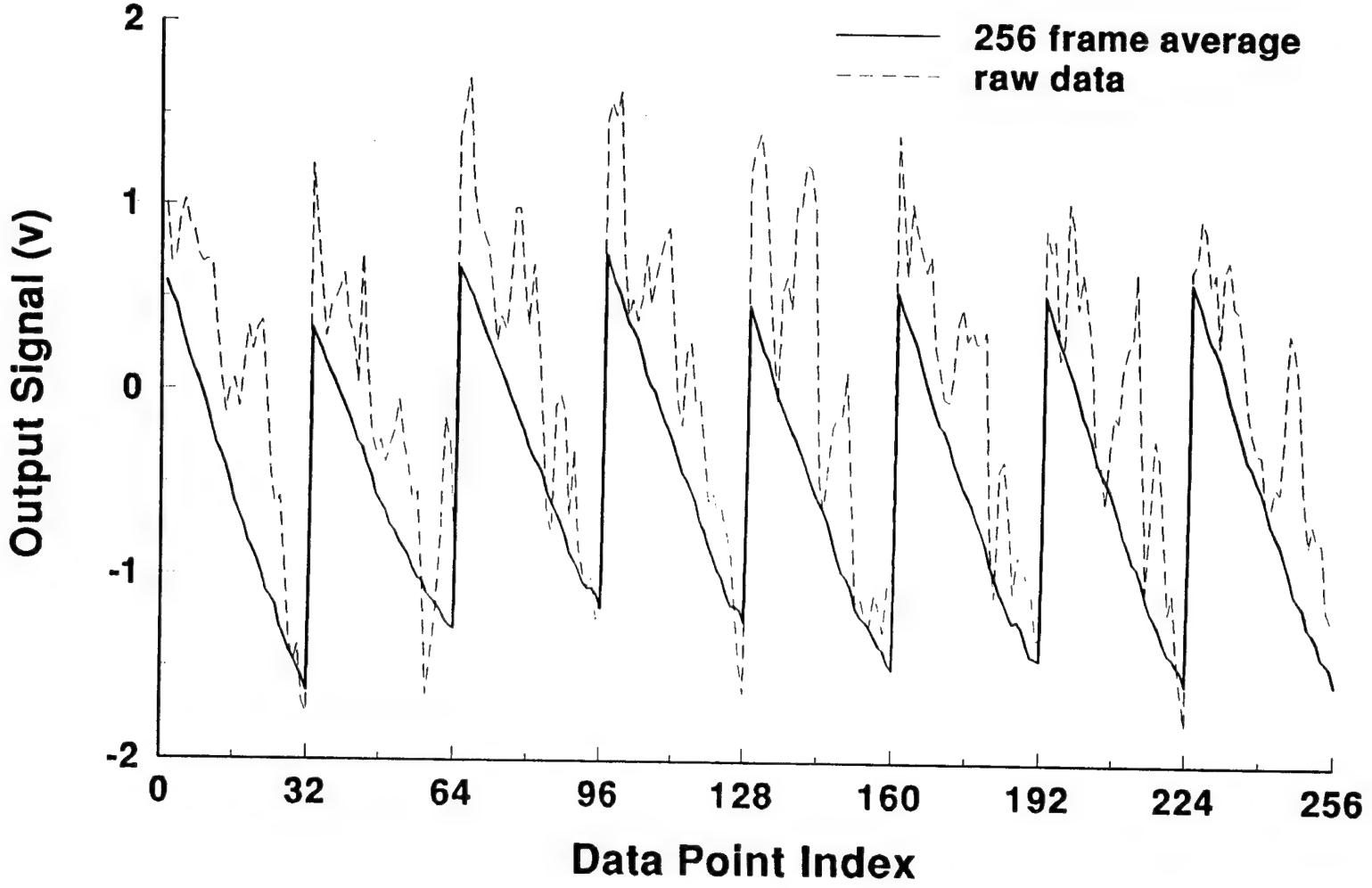

3. Single frame of open-ocean data from the position sensor and the pattern produced by the 9 s (256 frame) averaging procedure.

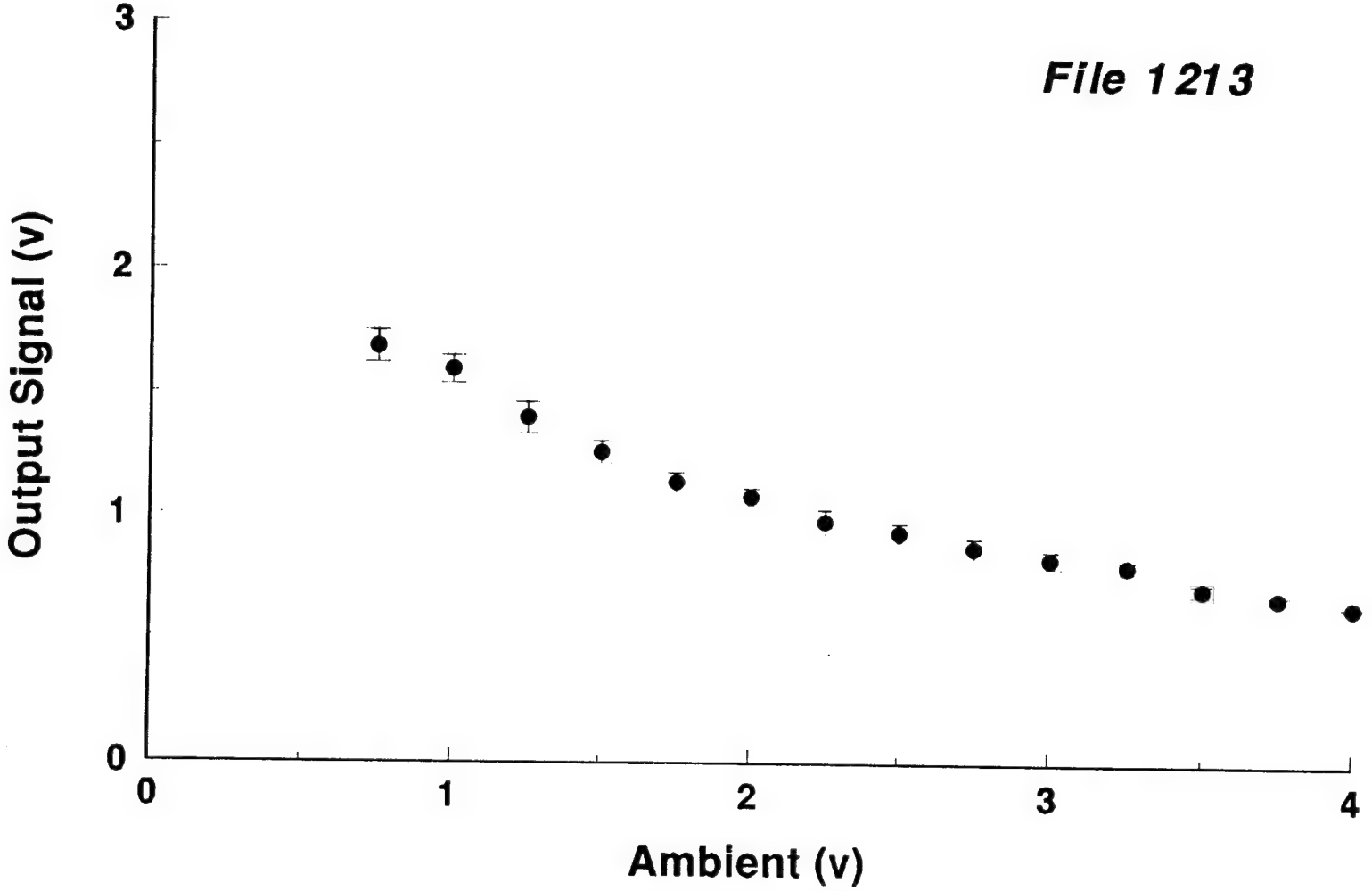

4a. Position sensor output signal vs ambient light intensity for an open-ocean deployment of the SSS system. The means and error bars were computed on the basis of 0.25 v (ambient level) bins.

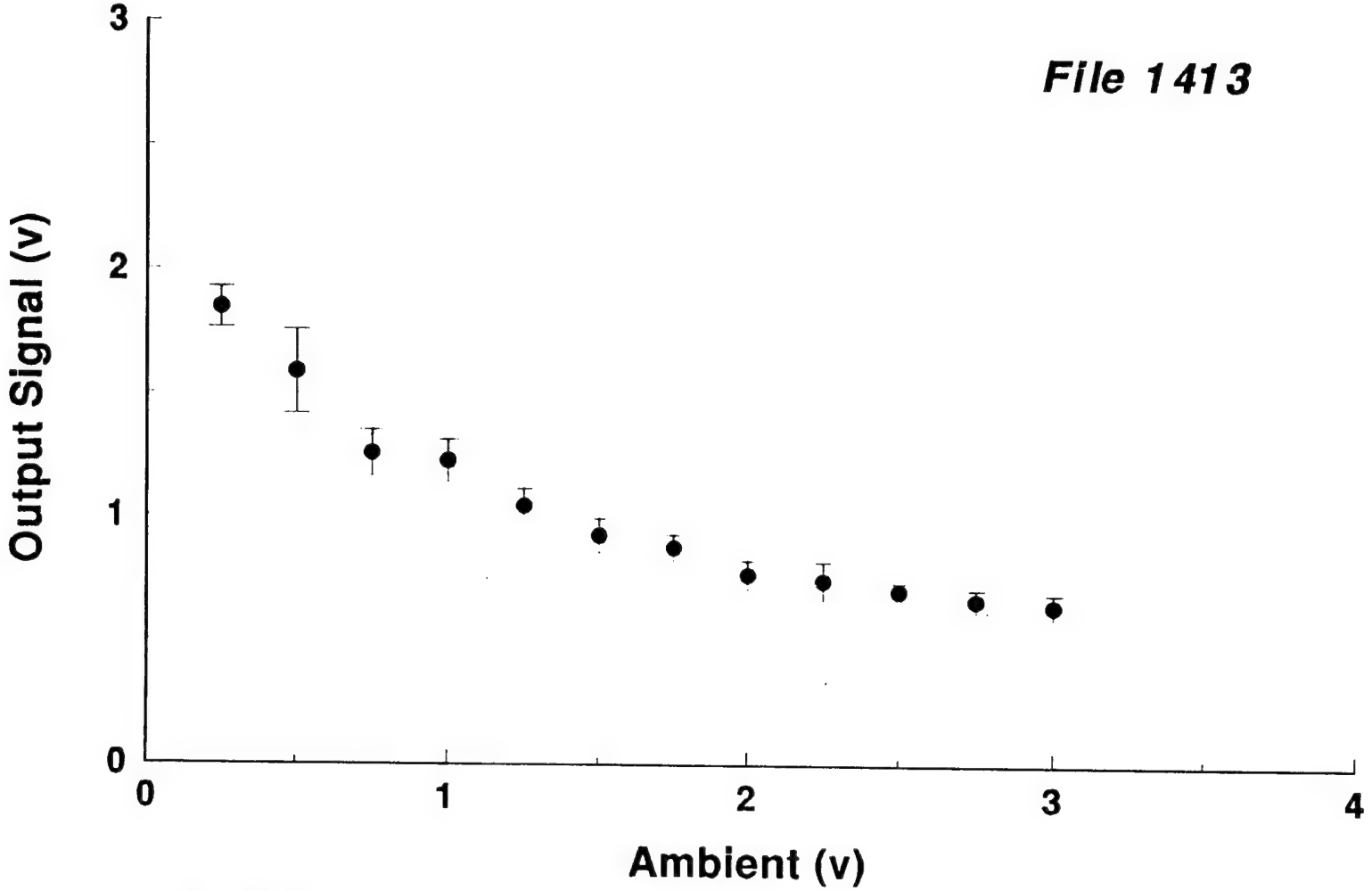

4b. Position sensor output signal vs ambient light intensity for an open-ocean deployment of the SSS system. The means and error bars were computed on the basis of 0.25 v (ambient level) bins.

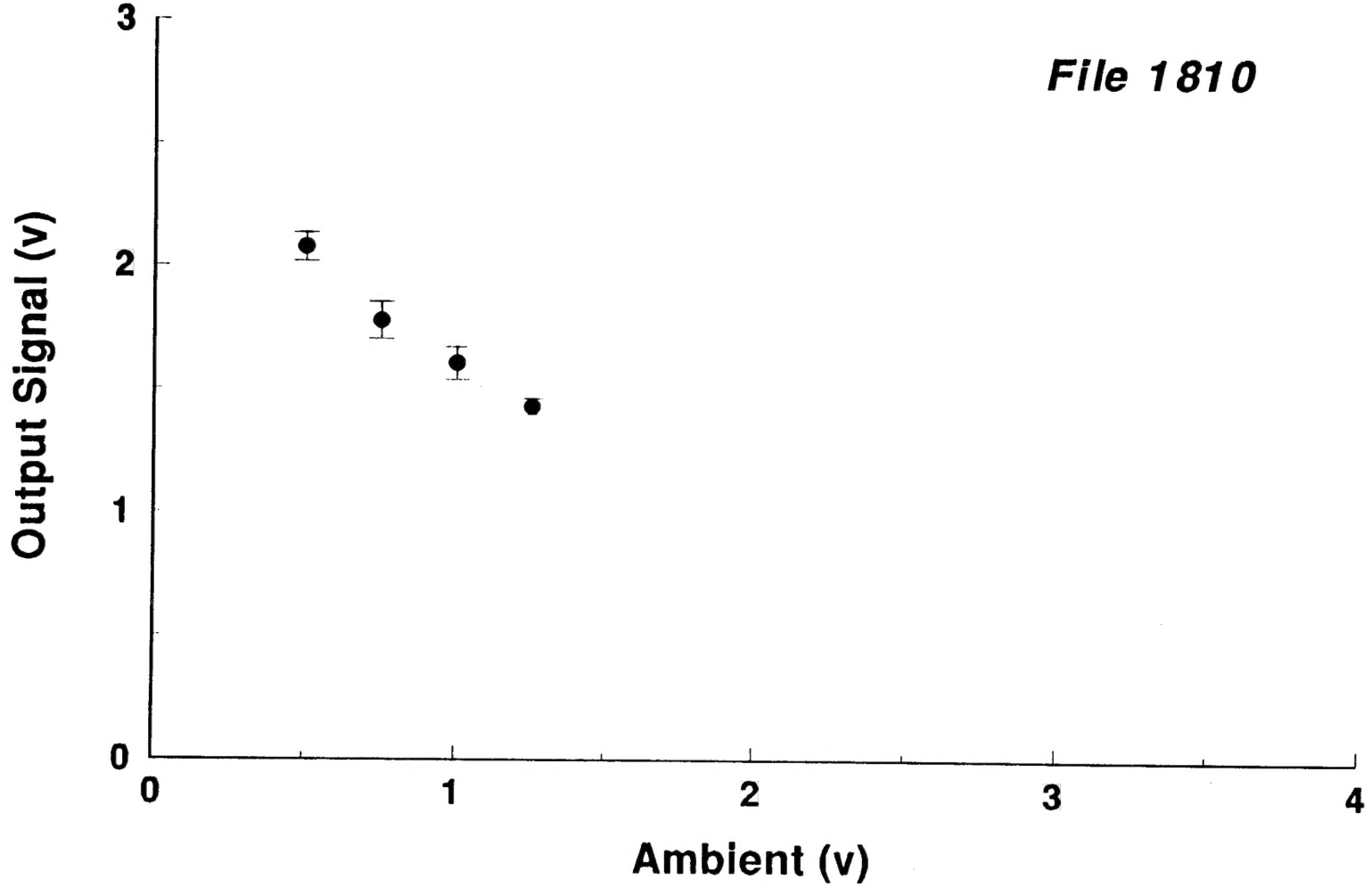

4c. Position sensor output signal vs ambient light intensity for an open-ocean deployment of the SSS system. The means and error bars were computed on the basis of 0.25 v (ambient level) bins.

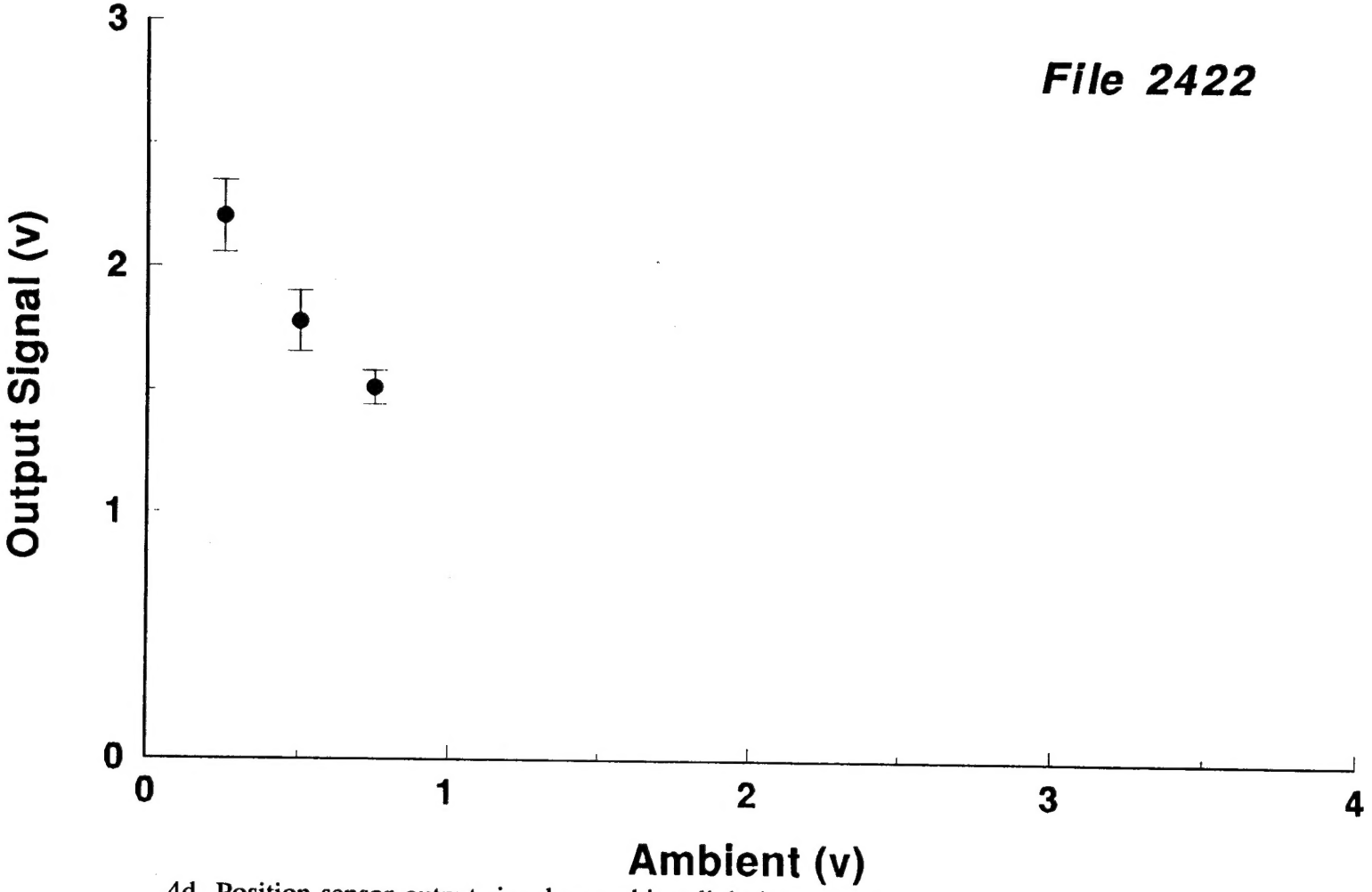

4d. Position sensor output signal vs ambient light intensity for an open-ocean deployment of the SSS system. The means and error bars were computed on the basis of 0.25 v (ambient level) bins.

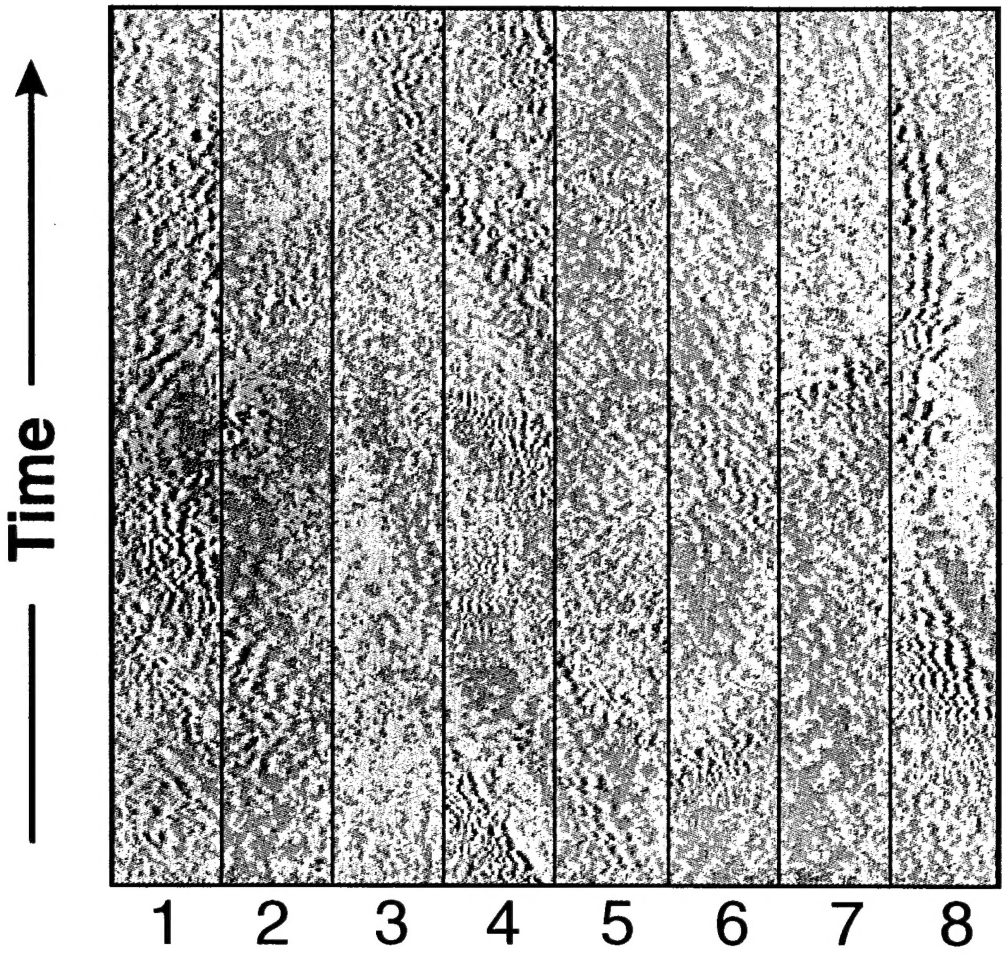

5. Typical grey-scale image of the surface curvature measured during the North Atlantic deployment. 256 contiguous frames are shown in the eight parallel columns.

a)

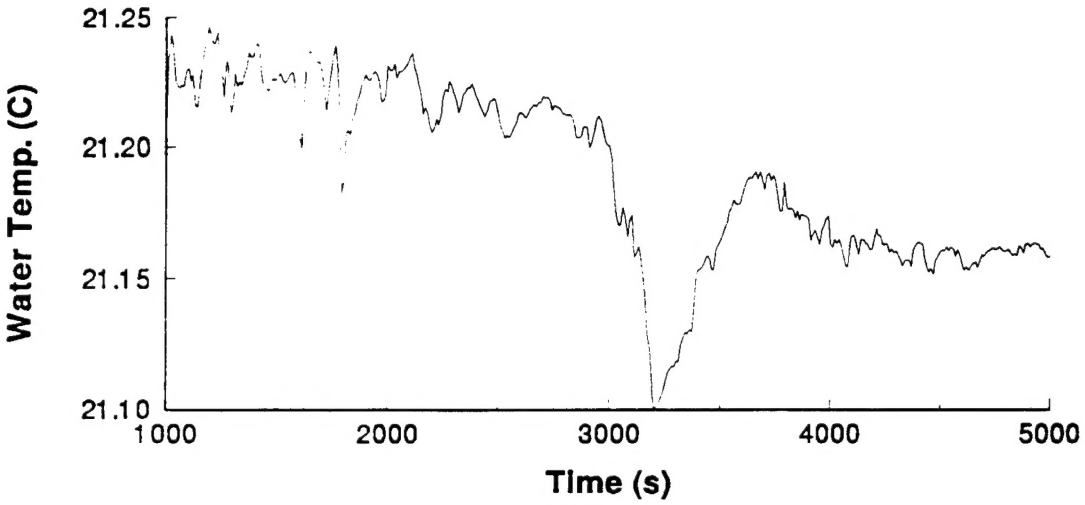

b)

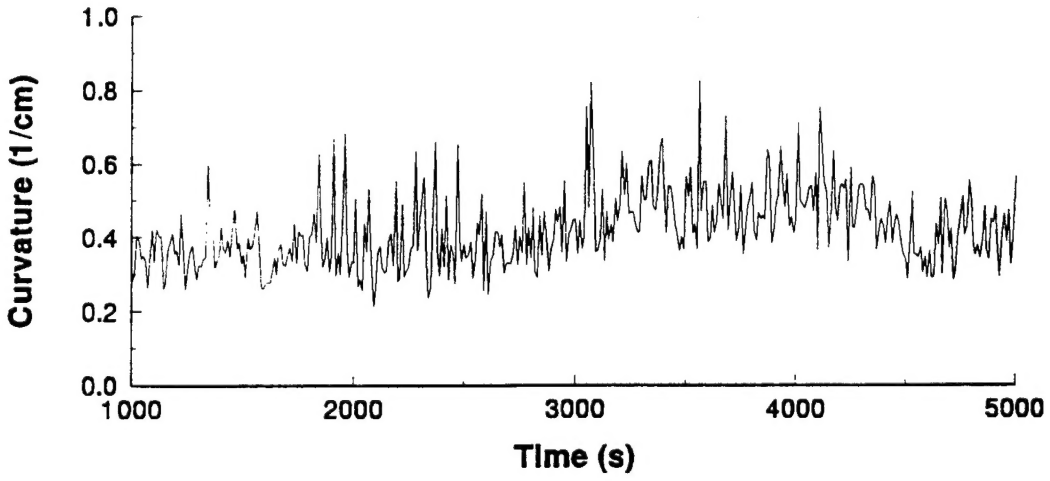

6. SSS system data collected in the presence of internal waves. a) Water temperature versus time, b) corresponding rms surface curvature.